Int. J. Electrochem. Sci., 15 **(2020)** 10674 – 10683, doi: 10.20964/2020.11.16

International Journal of
ELECTROCHEMICAL
SCIENCE
www.electrochemsci.org

Short Communication

One Step Preparation of Superhydrophobic Surface on Copper Substrate with Anti-Corrosion and Anti-Icing Performance

Hong Li[1,2,*], *Yanfeng Lu*[1], *XinYan Zou*[1], *Chunyu Wang*[1], *Hongyan Wei*[1]

[1] School of Physics and Electronic Information, Huaibei Normal University, Huaibei, 235000, PR China
[2] Schoo Key Laboratory of Green and Precise Synthetic Chemistry and Applications, Ministry of Education; Huaibei Normal University, Huaibei, Anhui 235000, P. R. China
[*]E-mail: lihonggreat@126.com

Received: 30 June 2020 / *Accepted:* 5 August 2020 / *Published:* 30 September 2020

Copper stearate coating was fabricated on a copper substrate through a simple solution immersion method at room temperature. The surface exhibited grass-like structure, which endowed it with superhydrophobicity and the water contact angle was about 152.3°. Electrochemical measurement revealed that this superhydrophobic surface (SHS) showed better corrosion resistance than bare copper surface and the inhibition efficiency of this SHS was about 95.91%. Moreover, the SHS demonstrated the reduction in adhesion between ice and surface, thus allowing for easy removal of ice. This method may provide a simple way to design SHS with corrosion resistance and anti-icing performance on metal surfaces.

Keywords: Copper stearate coating; Corrosion resistance; Electrochemical measurement; Anti-icing

1. INTRODUCTION

Superhydrophobic surface (SHS) has attracted significant research interest due to its wide range of applications in many fields, such as corrosion resistance surfaces [1–3], anti-icing surfaces [4,5], biomedical materials [6,7], microfluidic systems [8], etc. Noteworthy, rough structure and low surface energy [9–11] are of great importance for the formation of SHS as they usually decide the degree to which a solid repels a liquid. The SHS is usually achieved through a two-step process as follows: the rough structures are first prepared on solid surfaces, and then modified with materials having lower surface energy [12–14]. Therefore, it is speculated that the preparation of SHS can be greatly simplified if these two steps are combined into one [15].

Huge economic losses are caused every year due to metal corrosion [16]. Metal corrosion can ruin the integrity of the equipment, leading to safety issues and catastrophic failures. Till date, several

methods have been used to prevent metal corrosion [17–19]. Among these methods, formation of superhydrophobic film on the substrate metal is one of the most useful strategies to effectively slow down the metal corrosion [20]. Air trapped in the rough structure leads to the effective separation of the corrosive liquid from the metal surface. In recent years, significant research efforts have been devoted to fabricate these surfaces through various preparation methods, including: chemical vapor deposition [21], etching [22], hydrothermal method [23,24], pulsed laser deposition [25], sol–gel process [26], and so on. For example, Wan et al. [27] prepared SHS on the copper substrate by etching and hydrothermal methods. This SHS showed high corrosion inhibition efficiency and good stability.

Surface icing of metallic surfaces at low temperatures can also pose serious hazard because metal is the main material of aircraft, engines, ships, and refrigeration systems [28]. Preparation of anti-icing metal surface is a serious problem encountered globally. Mechanical or manual deicing and ice-over resistant coating are the methods that are often used nowadays. However, these methods have several disadvantages [29]. Generation of SHS has been believed to be a potential approach to realize effective anti–icing performance. It can reduce the adhesion between ice and surface, allowing the ice to fall off with less force or under its own gravity. Liao et al. fabricated ZnO/SiO_2/PTFE structure on glass substrate through magnetron sputtering. Results showed that this SHS exhibited excellent anti-icing performance [30].

In this study, SHS made of copper stearate coating was fabricated on copper substrates by a simple one step process. Copper substrates were immersed in ethanol solution of stearic acid for different times at room temperature. Electrochemical measurements were carried out, which revealed that the corrosion resistance of SHS was significantly improved. Moreover, anti-icing tests showed that ice on the surface of sample produced many cracks and it could fall off easily.

2. EXPERIMENTAL

2.1. Preparation of copper stearate coating on Copper substrate

First, Copper foils were cleaned by ultrasonication using ethanol. Then, the cleaned Copper foils were immersed into ethanol solution of stearic acid (8 mM) for 6, 12, 24, 72, and 120 h at room temperature, respectively. Finally, samples were dried in warm air. All reagents were purchased from Aladdin Company.

2.2. Sample characterization

The surface nanostructure and chemical composition of samples were measured by field emission scanning electron microscopy (FESEM, JEOL JSM-6610LV) and X-ray diffraction (XRD, Seifert, XDAL 3000). The water contact angle (WCA) on the surface of samples was measured using (JC2000C1. Shanghai). The potentiodynamic polarization curves and Nyquist plot were evaluated by electrochemical measurement (CHI 760E, Shanghai) using three-electrode system with silver chloride and graphite as reference electrode and counter electrode in 3.5 wt% NaCl solution. The samples with

bare area of 1 cm^2 serve as work electrode. The scanning rate of potentiodynamic polarization was 1 mv/s.

3. RESULTS AND DISCUSSION

3.1. Morphology, composition, and wettability

Fig. 1 shows FESEM images of nanostructures prepared on Copper substrate. When the soaking time is short (6 and 12 h), a few clusters of nanostructures can be found; however, the number of clusters is small (Figs. 1(a) and (b)). With the increase in the soaking time to 24 h, even 72 h, the density of clusters increases as shown in Figs. 1(c) and (d). The individual clusters are composed of emission nanosheets, and the morphology of grass-like cluster undergoes only a slight change with the increase of soaking time.

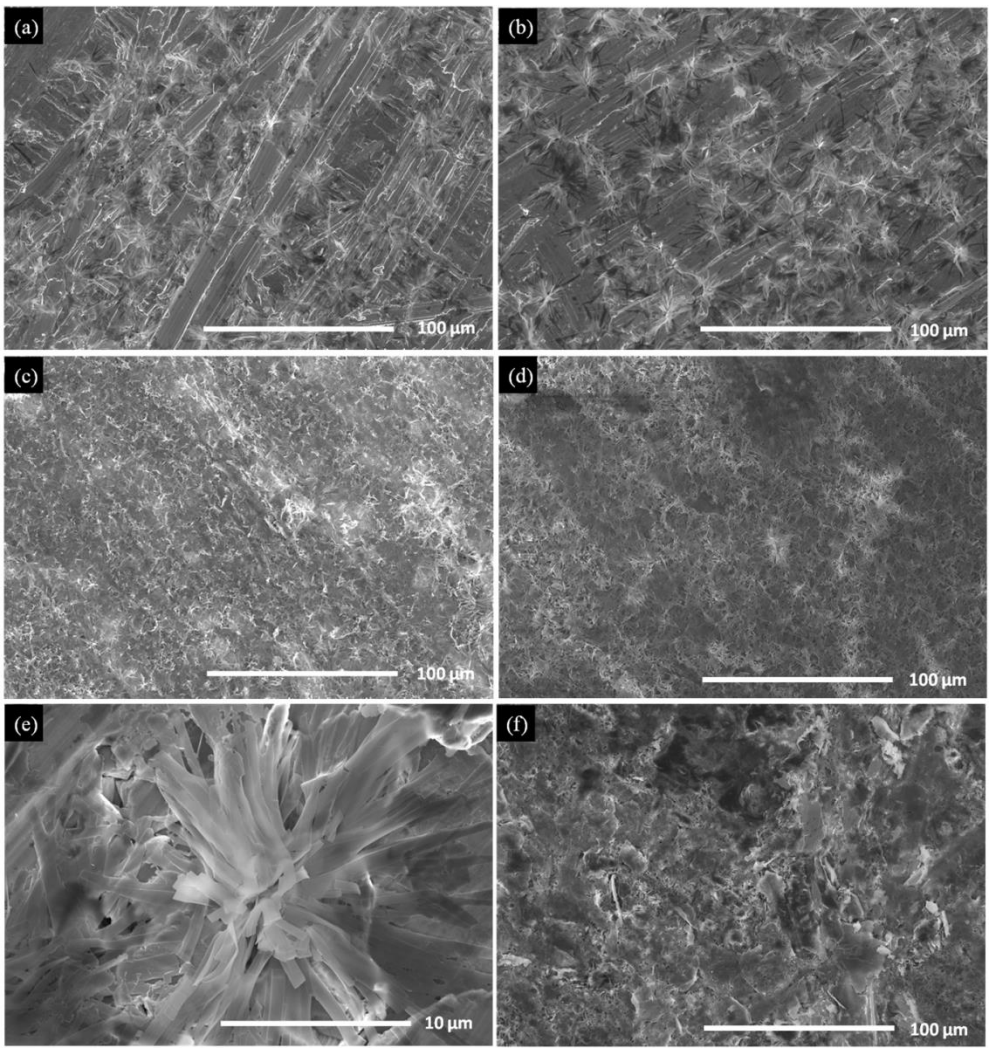

Figure 1. FESEM images of the as-prepared nanostructures on Copper substrate for different soaking time: (a) 6 h, (b) 12 h, (c) 24 h, (d) 72 h, and (f) 120 h, and (e) higher magnification image of a single cluster in (d).

Fig.1(e) shows that the length and width of nanosheets are about 10 and 1μm, respectively. When the soaking time is 120 h, the morphology of the surface gets destroyed. Fig.2 shows the XRD patterns of nanostructure prepared on the surface of Copper substrate for soaking time of 12 and 72 h, respectively.

The locations of the three peaks correspond to those of the copper stearate coating (JCPDS00-055-1622) [31]. Moreover, the intensity of copper stearate coating peaks increases with the increase of soaking time as confirmed from Fig. 1.

The oxidation process of Copper is very slow because the surface of Copper gets covered with an oxidized layer. However, this oxidation process gets accelerated in ethanol solution of stearic acid due to the acidic environment [12]. Cu^{2+} is produced in the solution according to the following reactions:

$$2Cu + O_2 + 4H^+ \rightarrow 2Cu^{2+} + 2H_2O$$

Cu^{2+} reacts with stearic acid to form copper stearate coating according to the following reaction:

$$Cu^{2+} + 2CH_3(CH_2)_{16}COOH \rightarrow Cu[CH_3(CH_2)_{16}COO]_2 + 2H^+$$

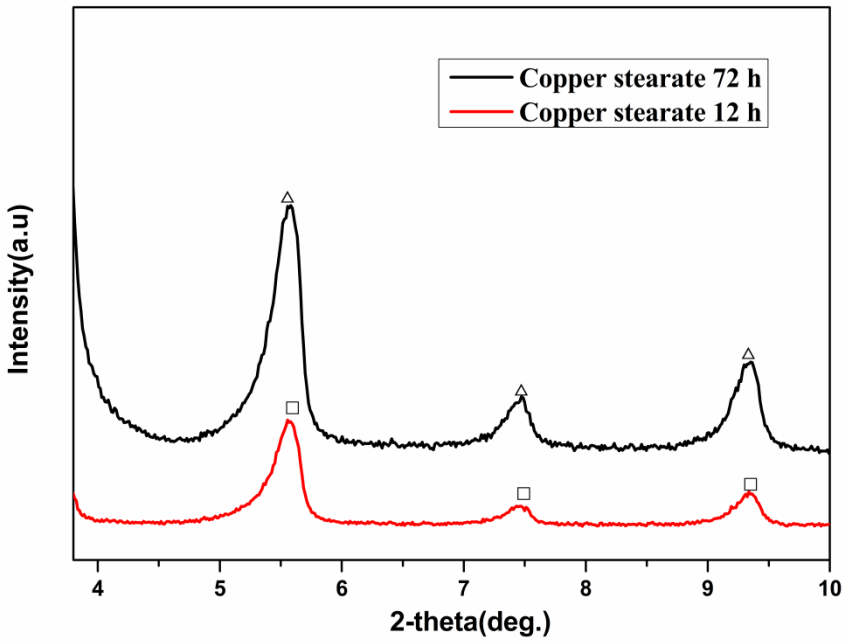

Figure 2. X-ray diffraction patterns of copper stearate coating prepared on the Copper surface for soaking time of 12 and 72 h, respectively.

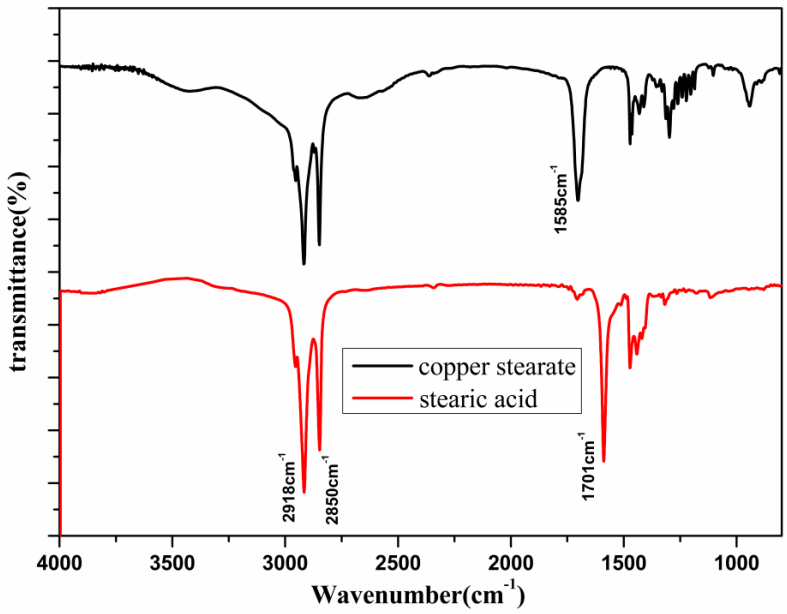

Figure 3. FTIR spectra of stearic acid and copper stearate coating with soaking time of 72 h.

These results indicated the successful fabrication of copper stearate coating on Copper substrate. With the progress of the reaction, more and more copper stearate coating grows on the surface of the Copper substrate. However, with the increase of soaking time, the surface morphology of copper stearate coating was destroyed due to the presence of hydrogen ions in the solution, as shown in Fig. 1(f).

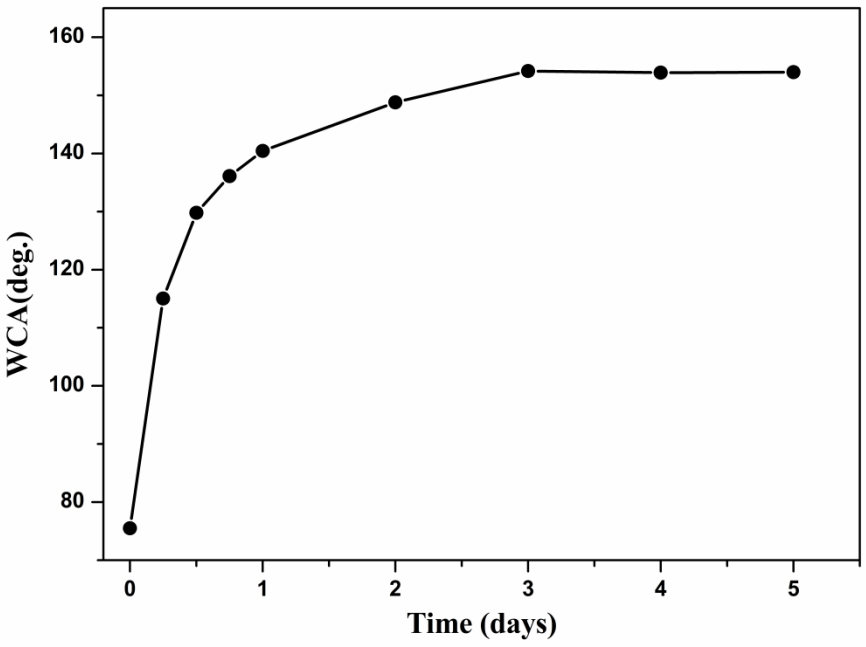

Figure 4. Relationship between WCA and soaking time.

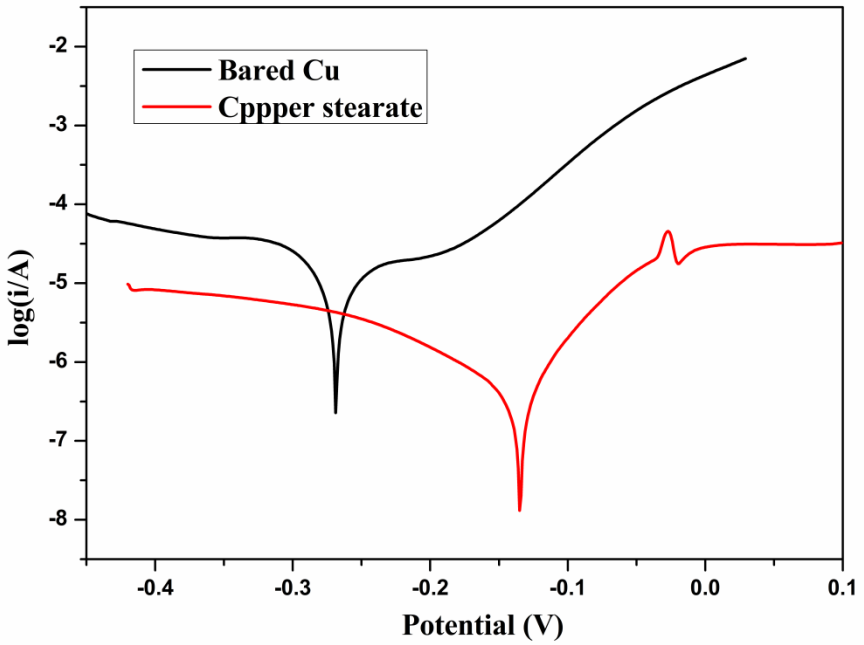

Figure 5. Potentiodynamic polarization curves of bare Copper and copper stearate coating after immersion in 3.5 wt% NaCl solution

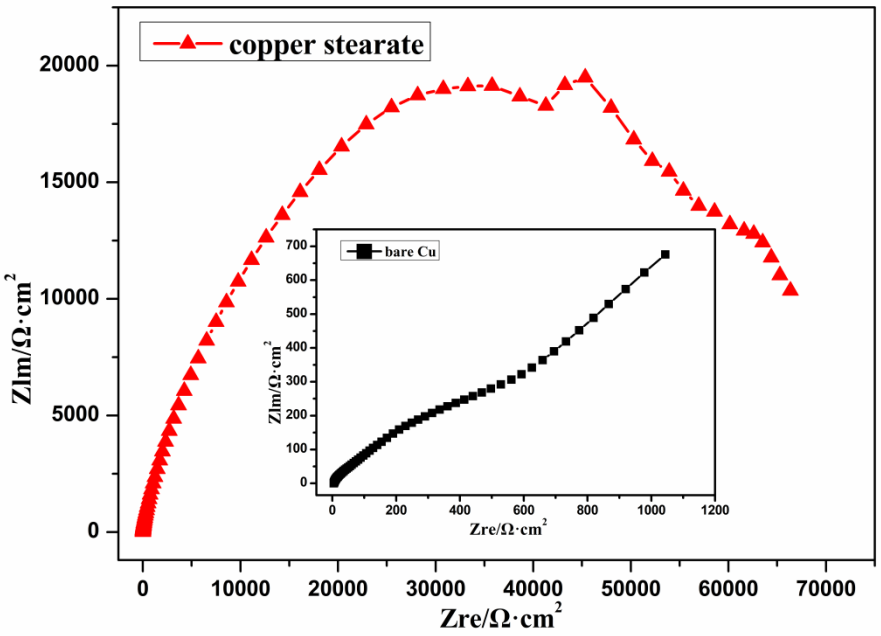

Figure 6. Nyquist curves of bare Copper and copper stearate coating after immersion in 3.5 wt% Nacl solution

Fig. 3 shows Fourier transform infrared (FTIR) spectra of stearic acid and copper stearate coating. Comparative analysis indicates that the absorption peak of stearic acid at 1701 cm^{-1} attributed to –COOH group disappears; instead, a peak at 1585 cm^{-1} corresponding to -COOH- groups appears,

indicating the successful fabrication of copper stearate coating on the surface of Copper substrate [32]. Two absorption peaks at 2918 cm^{-1} and 2850 cm^{-1} identical to those of stearic acid are attributed to the antisymmetric and symmetric stretching vibration of methyl and methylene, respectively [33]. This indicates that stearic acid is successfully coated on the surface of copper stearate coating.

The wettability of samples was evaluated based on WCA. Fig. 4 illustrates the relationship between the WCA and soaking time. Obviously, the soaking time significantly influences the WCA of samples. The WCA increases abruptly from 75.5° to 129.8° with the increase in the soaking time from 0 to 24 h and WCA reaches its maximum value of 152.3° when the soaking time is 72 h. With the further increase in the soaking time, the WCA decreases slightly. It can be shown that the WCA varies according to the density of clusters. According to Cassie equation

$$\cos\theta^* = -1 + f_1(1+\cos\theta)$$

With the increase of density of clusters, progressively more air is trapped in rough surface; thus the wettability of sample is superhydrophobic. The copper stearate coating with soaking time of 72 h is selected as the research object for the following study.

3.2. Electrochemical test

In general, Tafel curves and Nyquist plot are used to evaluate the protective effects of samples. Fig. 5 shows potentiodynamic polarization curves of bare Copper and copper stearate coating.

Table 1. Corresponding corrosion current density of bare Copper and copper stearate coating.

Sample	E_{corr} (mV)	i_{corr} (A cm^{-2})	η(%)
Copper	-0.267	6.789×10^{-6}	
Copper stearate coating	-0.135	2.777×10^{-7}	95.91

where i^0_{corr} and i_{corr} are corrosion current density of the bare Copper and copper stearate coating, respectively. The inhibition efficiency of copper stearate coating is about 95.91%. This indicates that the SHS composed of copper stearate coating can effectively reduce corrosion. Fig. 6 shows the Nyquist plot of bare Copper and superhydrophobic copper stearate coating. The Nyquist plot of bare Copper is composed of capacitive loop at high frequency and approximates straight line at low frequency. The capacitance diameter of bare Copper increases by two orders of magnitude after covering with copper stearate coating. This is consistent with the result shown in Fig. 5. This shows that the SHS composed of copper stearate coating has good barrier properties and can inhabit the penetration of sodium ions and chloride ions through the pores to the Copper substrate [34]. Xu et al. [24] fabricated SHSs on Al substrate in ethanolic stearic acid containing copper nitrite under 10 V DC voltage. Compared to the preparation method used in this study, method by Xu et al. is more complicated and tedious. Moreover, it did not provide the inhibition efficiency, which is important to analyze corrosion properties.

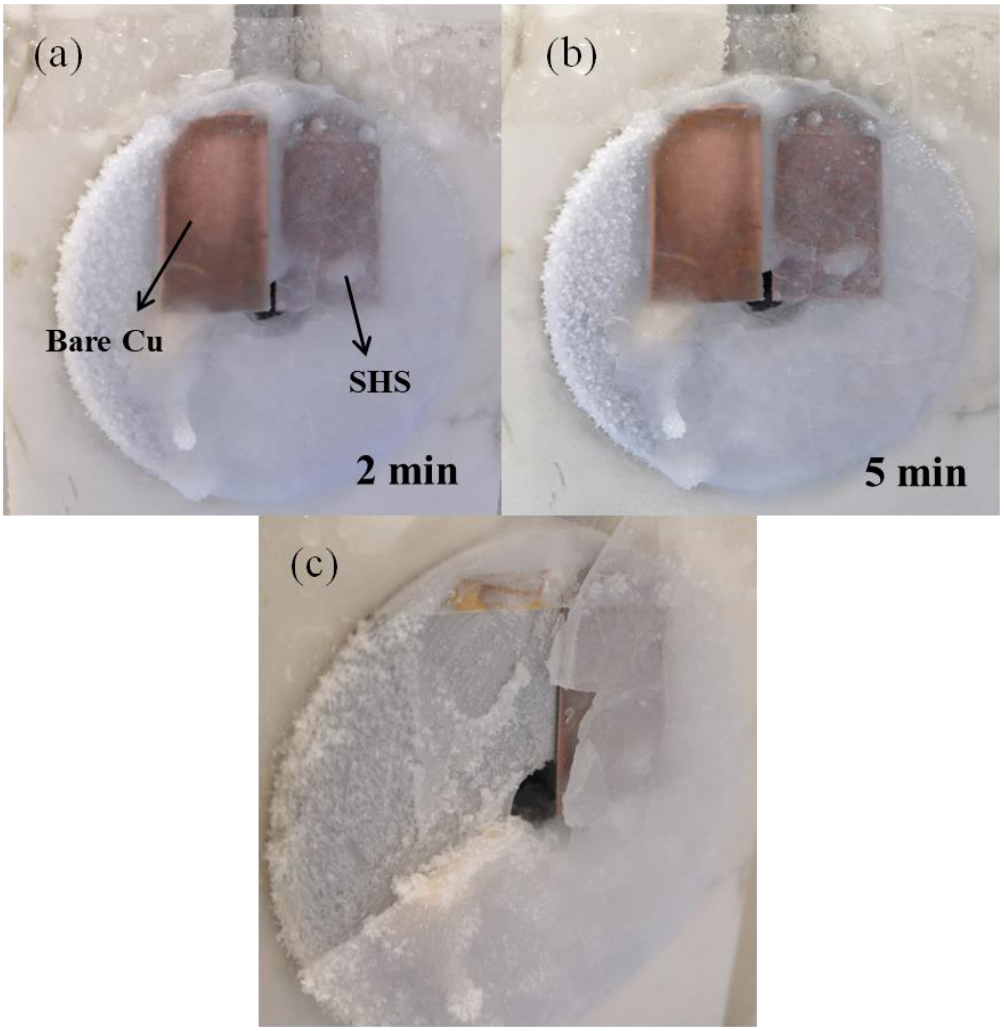

Figure 7. The freezing process of bare Copper and superhydropbobic surface of copper stearate coating.

Lower current density at a certain corrosion potential indicates lower electrochemical reaction activities and better corrosion resistance. Surface of copper stearate coating form passivation layer when corrosion potential is about -0.027 V, and the anodic current density is almost constant within the tested range (from 0 to 0.1 V). However, the anodic current density of bare Copper exhibits a rapid increase. Therefore, the surface of copper stearate coating exhibits positive corrosion potential and lower corrosion current density comparable to those of bare Copper. The reduced current density and positive voltage are attributed to air which is trapped between electrolyte and rough texture of copper stearate coating. The air acting as capacitor can separate sodium ions and chloride ions from Copper substrate [35]. Table 1 lists the corresponding electrochemical parameters. The inhibition efficiency can be calculated by using the following formula:

$$\eta = \frac{i_{corr}^{o} - i_{corr}}{i_{corr}^{o}}$$

3.3 Anti-icing property

Anti-icing property was investigated in an enclosed freezer set at a temperature of -10 ^{o}C. A small amount of water was sprayed on the surface of sample every 10 s. Fig. 7(a) illustrates that in 2 min two samples are fully covered with a thin layer of ice. The SHS is bright and full of cracks. When the incident angle is greater than the critical angle, the light incident from the ice to the air interface undergoes a total reflection. Thus, the bright surface shows that there is still a lot of air between the ice and the SHS, thus the adhesion between them is low. The surface of bare Copper is transparent, indicating that the adhesion between ice and bare Copper is high. When the freezing time is 5 min (Fig. 7(b)), the ice thickness on two samples surface increases, and the number of cracks on the SHS also gets enhanced. Fig. 7(c) demonstrates that most of the surface ice does not contact with the SHS. These results demonstrate the SHS has a certain anti-icing property.

4. CONCLUSION

Copper substrates were immersed in ethanol solution of stearic acid for different time at room temperature. The formation of rough structure of copper stearate coating and the adsorption of stearic acid were found to be responsible for the formation of SHS. Potentiodynamic polarization curves and Nyquist plot illustrated that this SHS exhibited better corrosion resistance compared to bare Copper. Anti-icing experiments showed that the contact area between ice and SHS was small, thus the ice could easily fall off.

ACKNOWLEDGEMENTS
This work was supported by the Natural Science Foundation (No.11974127, 51973078) and the Natural Science Foundation of Anhui Province (No:1808085ME140).

References

1. Y. Wan, M. Chen, W. Liu, X.X. Shen and Q. Xu, *Electrochim. Acta*, 270 (2018) 310.
2. Z. Qian, S.Wang, X.Ye, Z. Liu, and Z. Wu, *Appl. Surf. Sci*., 453 (2018) 1.
3. H. Zhu, W. Hu, S. Zhao, X. Zhang and Z. Wang, *J. Mater. Sci*. 55 (2020) 2215.
4. S. Barthwal and S.H. Lim, *Soft Matter*, 15 (2019) 7945.
5. S. Rajiv,S. Kumaran and M. Sathish, *J. Appl. Polym. Sci*., 136 (2019) 47059.
6. K.K. Chenab, B. Sohrabi, and A. Rahmanzadeh, Biomater Scu-uk, 7(2019) 3110.
7. M.C. Moran, G. Ruano, F. Cirisano and M. Ferrari, *Mat. Sci. Eng. C-mater*., 99 (2019) 241.
8. B. Bolteau, K. Dos Santos, F. Gelebart, J. Gomes, J. Teisseire, E. Barthel, and J. Fresnais, *Langmuir*, 35 (2019) 9133.
9. Cohen Céline, Y. Bouret, Y. Izmaylov, G. Sauder and X. Noblin,.*Soft Matter*,15 (2019)
10. T. Yeerken, G. Wang, H. Li, H.L. Liu and W.D. Yu, *Text. Res. J*., 89 (2019) 4827.
11. H.S. Maharana, A. Basu and K. Mondal, *Surf. Coat. Tech*., 375 (2019) 323.
12. S.T. Wang, L. Feng and L. Jiang, *Adv. Mater*., 18 (2006) 767.
13. H. Li, H.Y. Lu, S.L. Liu, Q. Li, Q.Z. Liu, SiO_2 shell on ZnO nanoflake arrays for UV-durable superhydrophobicity on Al substrate, *Mater. Res. Bull*., 114 (2019) 85-89.

14. B.Q.H. Nguyen, A. Shanmugasundaram, T.F. Hou, J. Park and D.W. Lee, *Chem. Eng. J*., 373 (2019) 68.
15. N. Saleema, D.K. Sarkar, R.W. Paynter and X.G. Chen, *ACS Appl. Mater. Inter*., 2 (2010) 2500.
16. H. Li, H.Y. Wei, X.Y. Zou, C.Y. Wang, Q. Gao, Q. Li, Q.Z. Liu and J.F. Zhang, *Mater. Chem. Phys.*, 246 (2020) 122839.
17. M.Kaseem, T. Hussain and Y.G. Ko, *J. Alloy. Compd*., 822 (2020) 153566.
18. B. Lyu, H.H. Liu, P.F. Li, D.G. Gao and J.Z. Ma, *J. Ind. Eng. Chem*., 80 (2019) 411.
19. H. Firouzi-Nerbin, F. Nasirpouri and E. Moslehifard, *J. Alloy. Compd*., 822 (2020) 153712.
20. P. wang, T.P. Li and D. Zhang, *Corrosion Science*, 128 (2017) 110.
21. S. Barthwal and S.H. Lim, *Soft Matter*, 15 (2019) 7945.
22. C.W. Schultz, C.L.W. Ng and H.Z. Yu, *ACS Appl. Mater. Inter*., 12 (2010) 3161.
23. D.L. Lai, G. Kong, X.C. Li and C.S. Che, *J. Nanosci. Nanotechno*., 19 (2019) 3919.
24. N. Xu, D.K. Sarkar, X-Grant. Chen, H. Zhang and W.P. Tong, *RSC Advances*, 6 (2013) 35466-35478.
25. R.A. Alawajji, G.K. Kannarpady and A.S. Biris, *Appl. Surf. Sci*., 444 (2018) 208.
26. T. Pirzada, Z. Ashrafi, W.Y. Xie and S.A. Khan, *Adv. Funct. Mater*., 30 (2019) 1907359.
27. Y.X. Wan, M.J. Chen, W. Liu, X.X. Shen, Y.L. Min and Q.J. Xu, *Electrochim. Acta*, 270 (2018) 310.
28. R.J. Liao, Z.P. Zuo, C. Guo, A.Y. Zhuang, X.T. Zhao and Y. Yuan, *Appl. Surf. Sci*., 356 (2015) 539.
29. Y.M. Yang, Y.N. Wang, X.F. Yuan, Y.H. Chen and L. Tan, *Neural Comput. Appl*., 22 (2013) 969.
30. R.J. Liao, C. Li, Y. Yuan, Y.Z. Duan and A.Y. Zhuang, *Mater. Lett*., 206 (2017) 109.
31. K.K. Meng, X. Tan and Z.H. Jiang, *Mater. Sci. Tech-lond.*, 35 (2019) 1.
32. S. Meth and C.N. Sukenik, *Thin Solid Films*, 425 (2003) 49.
33. Y.A. Wu, R.M.J. Jacobs, J.H. Warner, G.R. Williams and C.J. Wang, *Chem. Matter*., 23 (2011) 171.
34. B. Yin, L. Fang, A. Q. Tang, Q. L. Huang, J. Hu, J. H. Mao,G. Bai and H. Bai, *Appl. Surf. Sci*., 258 (2011) 580.
35. Y. Liu, J.D. Liu, S.Y. Li, Y.M. Wang, Z.W. Han and L.Q. Ren, *Colloids and Surfaces A: Physicochem. Eng. Aspects*, 466 (2015) 125.